Results of the Neutronics and Shielding Calculational Benchmark

M.E. Sawan

November 1995

UWFDM-999

Presented at the IAEA Advisory Group Meeting on "Completion of FENDL-1 and Start of FENDL-2", Del Mar, CA, 5–9 December 1995.

FUSION TECHNOLOGY INSTITUTE

UNIVERSITY OF WISCONSIN

MADISON WISCONSIN

RESULTS OF THE NEUTRONICS AND SHIELDING CALCULATIONAL BENCHMARK

Mohamed E. Sawan

Fusion Technology Institute
University of Wisconsin-Madison
1500 Engineering Drive
Madison, WI 53706

December 1995

UWFDM-999

Presented at the IAEA Advisory Group Meeting on "Completion of FENDL-1 and Start of FENDL-2," Del Mar, CA, 5-9 December 1995.

INTRODUCTION

During the IAEA Advisory Group Meeting on "Improved Evaluations and Integral Data Testing for FENDL" held in Garching, Germany in the period 12-16 September 1994, the Working Group II on "Experimental and Calculational Benchmarks on Fusion Neutronics for FENDL Validation" recommended that a calculational benchmark representative of the ITER design should be developed [1]. This benchmark problem can be used to assess the impact of transport codes, nuclear data evaluation, nuclear data processing, and multigroup structure on the flux and design relevant nuclear parameters (heating, damage, gas production) in a fusion reactor relevant configuration. The detailed description and specifications of the neutronics and shielding calculational benchmark were provided to the IAEA Nuclear Data Section and documented in the IAEA Nuclear Data Section Report INDC(NDS)-316 [2]. The radial build for the benchmark problem is given in Fig. 1. Only two sets of results were received. These are from the University of Wisconsin (M. Sawan) and TSI Research, Inc. (E. Cheng). These results are reported and analyzed here.

CALCULATIONAL APPROACH

In the UW calculations, the discrete ordinates one-dimensional, diffusion-accelerated, neutral particle transport code ONEDANT was used with the P_3S_8 approximation. On the other hand, the TSI calculations used the discrete ordinates one-dimensional code ANISN with the P_3S_8 approximation. Both calculations used the FENDL/E-1.0 [3] library processed into the 175n-42g multigroup library FENDL/MG by R. MacFarlane using NJOY [4] and the VITAMIN-E weight function. We used the TRANSX [5] code to generate two working libraries from FENDL/MG for use in the benchmark calculations. The libraries include the nuclear responses of interest such as nuclear heating, dpa, tritium production, helium production, and hydrogen production. One library has the same group structure as FENDL/MG (175n-42g) and the other is collapsed into a 46n-21g group structure using the VITAMIN-E weight function. In the TSI calculations, no collapsing of the multigroup nuclear data library was considered and the gas production results were obtained using the REAC*3 [6] library. Calculations were performed also by the UW using two other

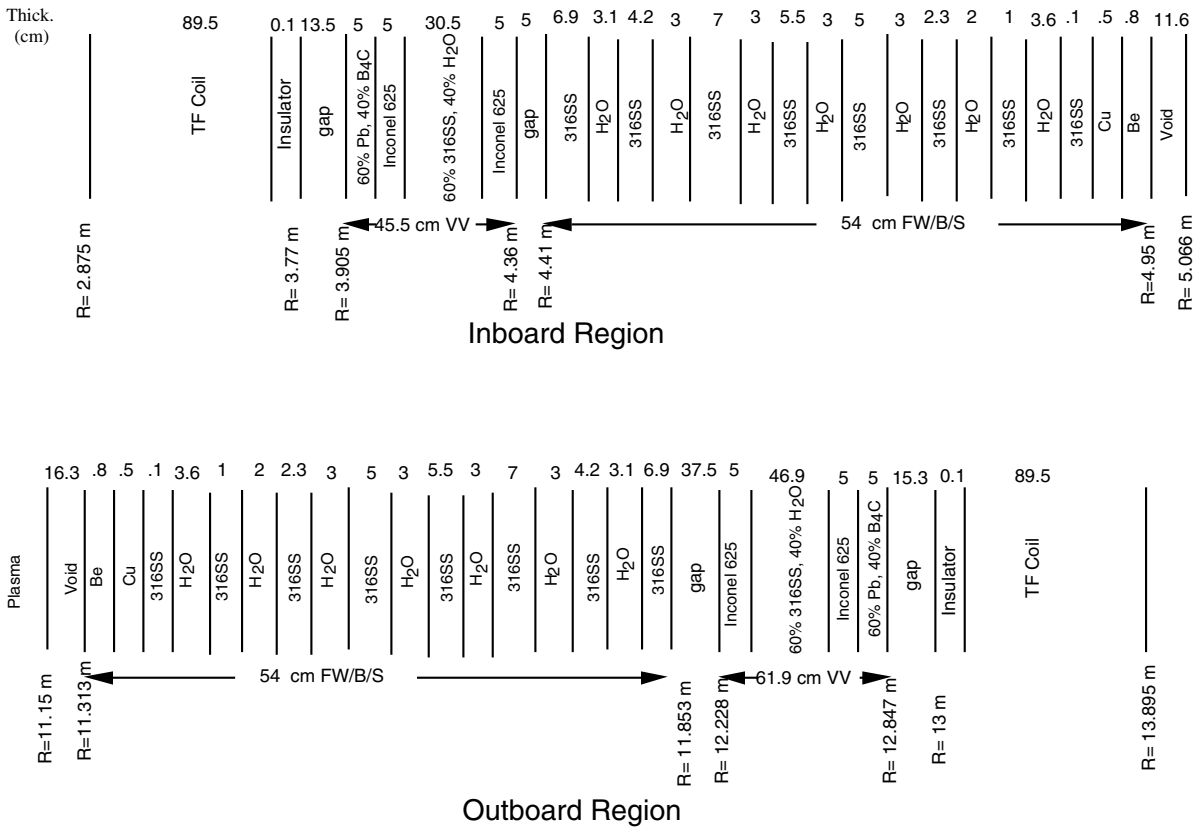

Fig.1. Radial build for the neutronics and shielding benchmark.

widely used libraries based on ENDF/B-V [7]. One library was generated using TRANSX from the MATXS5 library obtained by processing ENDF/B-V with NJOY. This library has a 30n-12g group structure. The other library has 46n-21g groups and is based on VITAMIN-E (processed from ENDF/B-V with the MINX [8] and AMPX [9] systems) for transport cross sections and KAOS/LIB [10] for nuclear responses. In the UW calculations, the 14.1 MeV neutron source is represented by placing it in the energy group that includes the 14.1 MeV energy. This corresponds to group 8 (13.84-14.191 MeV) for the 175 neutron energy group library, group 1 (13.499-14.918 MeV) for the 46 neutron energy group library, and group 2 (13.5-15 MeV) for the 30 neutron energy group library. However, in the TSI calculations, the 14.1 MeV neutron source is represented by a uniform distribution in groups 6-8 of the 175 n group library (13.84-14.918 MeV).

NEUTRON FLUX

Table 1 gives the peak neutron flux values obtained in the different calculations. Comparing the results based on FENDL to those based on ENDF/B-V using the same processing codes (NJOY/TRANSX), the neutron fluxes differ by <4% at the front of the blanket. The difference increases as one moves away from the blanket reaching ~8% at the magnet. The difference between the results based on FENDL with 175 and 46 neutron groups is very small. The results are almost identical in the first wall (FW) and the differences are less than ~3% at the vacuum vessel (VV) and magnet. Using the same 175 neutron group FENDL data, ANISN gives neutron flux results different from ONEDANT by 3-10%. Comparing the results based on FENDL to those based on ENDF/B-V with the same group structure using different processing codes (MINX/AMPX), the neutron fluxes differ by <3% at the front of the blanket. The difference increases as one moves away from the blanket reaching ~45% at the magnet.

GAMMA FLUX

Table 2 gives the peak gamma flux values obtained in the different calculations. Comparing the results based on FENDL to those based on ENDF/B-V using the same processing codes (NJOY/TRANSX), the gamma fluxes differ by <6% at the front of the blanket. The difference increases as one moves away from the blanket reaching ~20% at the VV. The difference between results based on FENDL with 175n-42g and 46n-21g group structures is very small (<2%). Using the same multigroup FENDL data, ANISN gives gamma flux results different from ONEDANT by <8%. The results are almost identical in the FW. Comparing the results based on FENDL to those based on ENDF/B-V with same group structure using different processing codes (MINX/AMPX), the gamma fluxes differ by ~17% at the front of the blanket. The difference increases as one moves away from the blanket reaching ~60% at the magnet.

NUCLEAR HEATING

The total nuclear heating (neutron and gamma) per cm height has been determined in the different zones. The results obtained using the different nuclear data libraries were compared.

Table 1. Peak Neutron Flux Values (n/cm^{2}s)

	UW	UW	UW	UW	TSI
Transport Code	ONEDANT	ONEDANT	ONEDANT	ONEDANT	ANISN
Evaluation	FENDL/E-1.0	FENDL/E-1.0	ENDF/B-V	ENDF/B-V	FENDL/E-1.0
Processing Code	NJOY TRANSX	NJOY TRANSX	NJOY TRANSX	MINX AMPX, KAOS	NJOY TRANSX
Energy Groups	175n-42g	46n-21g	30n-12g	46n-21g	175n-42g
<u>INBOARD</u>					
First Wall					
Be	3.445×10^{14}	3.447×10^{14}	3.551×10^{14}	3.549×10^{14}	3.57×10^{14}
Cu	3.076×10^{14}	3.080×10^{14}	3.174×10^{14}	3.173×10^{14}	3.28×10^{14}
SS	2.918×10^{14}	2.922×10^{14}	3.011×10^{14}	3.009×10^{14}	3.03×10^{14}
Vacuum Vessel	9.775×10^{11}	9.445×10^{11}	9.276×10^{11}	1.060×10^{12}	1.04×10^{12}
Magnet	2.428×10^{9}	2.367×10^{9}	2.492×10^{9}	3.227×10^{9}	2.64×10^{9}
<u>OUTBOARD</u>					
First Wall					
Be	4.115×10^{14}	4.116×10^{14}	4.227×10^{14}	4.218×10^{14}	3.96×10^{14}
Cu	3.774×10^{14}	3.776×10^{14}	3.873×10^{14}	3.868×10^{14}	3.72×10^{14}
SS	3.619×10^{14}	3.620×10^{14}	3.711×10^{14}	3.705×10^{14}	3.61×10^{14}
Vacuum Vessel	1.352×10^{12}	1.311×10^{12}	1.293×10^{12}	1.467×10^{12}	1.33×10^{12}
Magnet	3.567×10^{8}	3.515×10^{8}	3.767×10^{8}	5.090×10^{8}	3.89×10^{8}

Table 2: Peak Gamma Flux Values (g/cm^{2}s)

	UW	UW	UW	UW	TSI
Code	ONEDANT	ONEDANT	ONEDANT	ONEDANT	ANISN
Evaluation	FENDL/E-1.0	FENDL/E-1.0	ENDF/B-V	ENDF/B-V	FENDL/E-1.0
Processing Code	NJOY TRANSX	NJOY TRANSX	NJOY TRANSX	MINX AMPX, KAOS	NJOY TRANSX
Energy Groups	175n-42g	46n-21g	30n-12g	46n-21g	175n-42g
<u>INBOARD</u>					
First Wall					
Be	2.91×10^{14}	2.88×10^{14}	2.80×10^{14}	3.37×10^{14}	2.92×10^{14}
Cu	2.82×10^{14}	2.77×10^{14}	2.67×10^{14}	3.23×10^{14}	2.82×10^{14}
SS	2.79×10^{14}	2.74×10^{14}	2.61×10^{14}	3.15×10^{14}	2.80×10^{14}
Vacuum Vessel	5.48×10^{11}	5.39×10^{11}	4.56×10^{11}	6.91×10^{11}	5.64×10^{11}
Magnet	6.29×10^{8}	6.2×10^{8}	5.80×10^{8}	9.52×10^{8}	6.80×10^{8}
<u>OUTBOARD</u>					
First Wall					
Be	3.30×10^{14}	3.27×10^{14}	3.22×10^{14}	3.84×10^{14}	3.31×10^{14}
Cu	3.25×10^{14}	3.20×10^{14}	3.12×10^{14}	3.74×10^{14}	3.26×10^{14}
SS	3.27×10^{14}	3.22×10^{14}	3.11×10^{14}	3.71×10^{14}	3.29×10^{14}
Vacuum Vessel	7.43×10^{11}	7.33×10^{11}	6.22×10^{11}	9.39×10^{11}	7.69×10^{11}
Magnet	9.42×10^{7}	9.43×10^{7}	8.90×10^{7}	1.52×10^{8}	1.04×10^{8}

Comparing the results based on FENDL to those based on ENDF/B-V using the same processing codes (NJOY/TRANSX), the nuclear heating values differ by 3-6% in the FW with the largest difference being in the Cu layer. The differences in the blanket zones are <2%. In the VV, the differences are <3%. The difference is largest (~30%) in the Pb/B_4C back layer. Total nuclear heating results in the TF magnets differ by ~5% in the inboard region and ~8% in the outboard region. The difference between the results based on FENDL with 175n-42g and 46n-21g group structures is very small. The results are almost identical (<2%) with the largest difference in the VV. Using the same multigroup FENDL data, ANISN gives nuclear heating results identical to those from ONEDANT in the FW and the front layers of the blanket. The differences increase as one moves toward the magnet reaching ~10%. The KAOS library based on ENDF/B-V gives nuclear heating higher than the FENDL library processed by NJOY with the same group structure. The heating is higher by ~1% in Be, ~21% in Cu and ~10% in SS of FW. The total heating is higher by up to ~17% in the blanket, ~40% in Inconel of VV and ~60% in magnet. The higher heating is partially attributed to the inclusion of the decay energy in the KAOS library.

Table 3 gives the peak power density in the FW, blanket, VV, and magnet. The FW power density results based on FENDL and ENDF/B-V using the same processing codes (NJOY/TRANSX) differ by ~5% in Be, ~6% in Cu and ~3% in SS. The differences are <3 for the VV and magnet. The results based on FENDL with 175n-42g and 46n-21g group structures are almost identical with differences <1%. Using the same multi-group FENDL data ANISN gives peak power density results identical to those from ONEDANT in the FW and blanket. The differences are ~4% in the VV and ~10% in the magnet. The KAOS library based on ENDF/B-V gives higher peak power densities than the FENDL library processed by NJOY with the same group structure. The results are higher by ~1% in Be, ~21% in Cu and ~10% in SS of the FW. The results are higher by ~21% in the VV and ~54% in the magnet. The higher heating is partially attributed to the inclusion of the decay energy in the KAOS library.

The peak nuclear heating was calculated using two kerma factors provided in the KAOS library to assess the impact of neglecting the decay energy of short lived radionuclides. One of

Table 3. Peak Power Density Values (W/cm^3)

Code	UW ONEDANT	UW ONEDANT	UW ONEDANT	UW ONEDANT	TSI ANISN
Evaluation	FENDL/E-1.0	FENDL/E-1.0	ENDF/B-V	ENDF/B-V	FENDL/E-1.0
Processing Code	NJOY TRANSX	NJOY TRANSX	NJOY TRANSX	MINX AMPX,KAOS	NJOY TRANSX
Energy Groups	175n-42g	46n-21g	30n-12g	46n-21g	175n-42g
INBOARD					
First Wall					
Be	1.06×10^{1}	1.06×10^{1}	1.01×10^{1}	1.07×10^{1}	1.07×10^{1}
Cu	2.08×10^{1}	2.08×10^{1}	2.19×10^{1}	2.53×10^{1}	2.09×10^{1}
SS	1.82×10^{1}	1.82×10^{1}	1.87×10^{1}	2.01×10^{1}	1.84×10^{1}
Vacuum Vessel	3.32×10^{-2}	3.28×10^{-2}	3.18×10^{-2}	3.97×10^{-2}	3.42×10^{-2}
Magnet	3.07×10^{-5}	3.05×10^{-5}	3.09×10^{-5}	4.46×10^{-5}	3.33×10^{-5}
OUTBOARD					
First Wall					
Be	1.36×10^{1}	1.35×10^{1}	1.30×10^{1}	1.36×10^{1}	1.38×10^{1}
Cu	2.50×10^{1}	2.49×10^{1}	2.64×10^{1}	3.04×10^{1}	2.50×10^{1}
SS	2.21×10^{1}	2.21×10^{1}	2.28×10^{1}	2.44×10^{1}	2.24×10^{1}
Vacuum Vessel	4.47×10^{-2}	4.44×10^{-2}	4.32×10^{-2}	5.36×10^{-2}	4.64×10^{-2}
Magnet	4.53×10^{-6}	4.57×10^{-6}	4.70×10^{-6}	7.04×10^{-6}	5.02×10^{-6}

these includes the decay energy carried by gamma and beta emitted from decay of short lived (half life < 1 day) radionuclides. The results are given in Table 4. Since nuclear heating is dominated by gamma heating, the underestimate in total nuclear heating is small. Neglecting decay energy results in underestimating the power densities by ~2% in Be, ~10% in Cu and ~4% in SS of the FW. The underestimate is <1% in the Inconel VV and <2% in the TF coil. The differences between the peak power densities with the FENDL library processed by NJOY and the KAOS library based on ENDF/B-V are still large even with the decay energy neglected in the KAOS library. The differences are ~1% in Be, ~11% in Cu and ~6% in SS of the FW. The differences are ~20% in the VV and ~51% in the magnet.

RADIATION DAMAGE

Table 5 gives the peak end-of-life atomic displacement damage (dpa) in the FW and VV. The FW dpa results based on FENDL and ENDF/B-V using the same processing codes (NJOY/TRANSX) differ by ~5% in Cu and ~2% in SS. The difference in the peak dpa in the

Table 4. Impact of Neglecting Decay Heat on Peak Power Density Values (W/cm^3)

Evaluation	ENDF/B-V	ENDF/B-V
Processing Code	MINX, AMPX, KAOS	MINX, AMPX, KAOS
Energy Groups	46n-21g	46n-21g
Decay Energy	yes	no
INBOARD		
First Wall		
Be	1.07×10^{1}	1.05×10^{1}
Cu	2.53×10^{1}	2.30×10^{1}
SS	2.01×10^{1}	1.92×10^{1}
Vacuum Vessel	3.97×10^{-2}	3.95×10^{-2}
Magnet	4.46×10^{-5}	4.36×10^{-5}
OUTBOARD		
First Wall		
Be	1.36×10^{1}	1.34×10^{1}
Cu	3.04×10^{1}	2.77×10^{1}
SS	2.44×10^{1}	2.34×10^{1}
Vacuum Vessel	5.36×10^{-2}	5.33×10^{-2}
Magnet	7.04×10^{-6}	6.89×10^{-6}

Table 5. Peak End-of-Life dpa in FW and VV (dpa @ 3 FPY)

Code	UW ONEDANT	UW ONEDANT	UW ONEDANT	UW ONEDANT	TSI ANISN
Evaluation	FENDL/E-1.0	FENDL/E-1.0	ENDF/B-V	ENDF/B-V	FENDL/E-1.0
Processing Code	NJOY TRANSX	NJOY TRANSX	NJOY TRANSX	MINX AMPX,KAOS	NJOY TRANSX
Energy Groups	175n-42g	46n-21g	30n-12g	46n-21g	175n-42g
INBOARD					
First Wall					
Cu	28.2	28.1	29.2	29.7	31.0
SS	26.5	26.5	27.1	27.2	25.1
Vacuum Vessel	3.88×10^{-2}	3.83×10^{-2}	3.91×10^{-2}	4.69×10^{-2}	4.08×10^{-2}
OUTBOARD					
First Wall					
Cu	38.5	38.4	39.8	40.4	41.9
SS	36.9	36.8	37.4	37.7	34.6
Vacuum Vessel	5.32×10^{-2}	5.27×10^{-2}	5.40×10^{-2}	6.43×10^{-2}	5.64×10^{-2}

Table 6. Peak End-of-Life Helium Production in FW and VV (appm @ 3 FPY)

	UW	UW	UW	TSI
Code	ONEDANT	ONEDANT	ONEDANT	ANISN
Evaluation	FENDL/E-1.0	FENDL/E-1.0	ENDF/B-V	FENDL/E-1.0
Processing Code	NJOY TRANSX	NJOY TRANSX	MINX AMPX,KAOS	NJOY TRANSX
Energy Groups	175n-42g	46n-21g	46n-21g	175n-42g
INBOARD				
First Wall				
Be	1.30×10^{4}	1.30×10^{4}	1.37×10^{4}	1.67×10^{4}
Cu	7.02×10^{2}	7.07×10^{2}	7.80×10^{2}	9.29×10^{2}
SS	6.02×10^{2}	6.02×10^{2}	6.41×10^{2}	4.33×10^{2}
Vacuum Vessel	3.61×10^{-1}	3.57×10^{-1}	5.44×10^{-1}	3.36×10^{-1}
OUTBOARD				
First Wall				
Be	1.73×10^{4}	1.73×10^{4}	1.81×10^{4}	1.93×10^{4}
Cu	9.72×10^{2}	9.70×10^{2}	1.08×10^{3}	1.01×10^{3}
SS	7.89×10^{2}	7.88×10^{2}	8.41×10^{2}	5.57×10^{2}
Vacuum Vessel	4.88×10^{-1}	4.83×10^{-1}	7.36×10^{-1}	4.04×10^{-1}

Inconel VV is ~2%. The peak dpa results based on FENDL with 175n-42g and 46n-21g group structures are almost identical in the FW and VV (<1% difference). Using the same multigroup FENDL data, ANISN gives peak dpa results different from ONEDANT by ~10% in the Cu FW, ~7% in the SS FW and ~6% in the Inconel VV. The differences are attributed to differences in the calculated flux and the displacement energy used to calculate the dpa cross sections from the damage energy cross sections provided in FENDL/MG. While the data used by TSI assumed 40 eV for all constituent elements, the UW data used the values listed in the TRANSX report.

The KAOS library based on ENDF/B-V gives higher dpa values than the FENDL library processed by NJOY with the same group structure. The results are higher by ~6% in Cu FW, ~3% in SS FW and ~22% in the Inconel VV.

GAS PRODUCTION

The peak end-of-life gas production values (helium, hydrogen and tritium) in the FW and VV have been calculated. Table 6 gives the results for helium (He) production. The peak He production results based on FENDL with 175n-42g and 46n-21g group structures are almost

identical in the FW and VV (<1% difference). Using the same multigroup FENDL data, ANISN gives peak He production results different from ONEDANT by as high as ~42% in the FW and ~20% in the Inconel VV. The differences are attributed to differences in gas production cross sections used. While the TSI calculation uses REAC*3 data, the UW calculations use the partial cross section data in FENDL/MG. The KAOS library based on ENDF/B-V gives higher He production values than the FENDL library processed by NJOY with the same group structure. The results for the FW are higher by ~5% in Be, ~11% in Cu, ~7% in SS. The peak Inconel VV He production is higher by ~52%.

Table 7 gives the peak hydrogen (H) production results. The peak H production results based on FENDL with 175n-42g and 46n-21g group structures are almost identical in the FW and VV (<2% difference). Using the same multigroup FENDL data, ANISN gives peak H production results different from ONEDANT by as much as a factor of ~3 in the FW and ~30% in the Inconel VV. The differences are attributed to differences in gas production cross sections used in the TSI calculation. The KAOS library based on ENDF/B-V gives H production values different than the FENDL library processed by NJOY with the same group structure. The results for the FW are different by ~5% in Be, ~4% in Cu, ~13% in SS. The peak Inconel VV H production is higher by ~20%.

Table 8 gives the peak tritium (T) production results. The peak T production results based on FENDL with 175n-42g and 46n-21g group structures are almost identical in the FW and VV (<2% difference). Using the same multigroup FENDL data, ANISN gives peak T production results different from ONEDANT by as much as a factor of ~2 in the FW and a factor of ~6 in the Inconel VV. The differences are attributed to differences in gas production cross sections used in the TSI calculation. The KAOS library based on ENDF/B-V gives T production values different than the FENDL library processed by NJOY with the same group structure. The results for the the FW are different by ~5% in Be, ~3% in Cu, and ~72% in SS. The peak T production in the Inconel VV is higher by a factor of ~26.

Table 7. Peak End-of-Life Hydrogen Production in FW and VV (appm @ 3 FPY)

	UW	UW	UW	TSI
Code	ONEDANT	ONEDANT	ONEDANT	ANISN
Evaluation	FENDL/E-1.0	FENDL/E-1.0	ENDF/B-V	FENDL/E-1.0
Processing Code	NJOY TRANSX	NJOY TRANSX	MINX AMPX,KAOS	NJOY TRANSX
Energy Groups	175n-42g	46n-21g	46n-21g	175n-42g
INBOARD				
First Wall				
Be	1.73×10^{2}	1.69×10^{2}	1.78×10^{2}	3.92×10^{2}
Cu	2.15×10^{3}	2.16×10^{3}	2.08×10^{3}	7.60×10^{2}
SS	1.99×10^{3}	1.98×10^{3}	1.75×10^{3}	1.39×10^{3}
Vacuum Vessel	2.33	2.32	2.78	2.03
OUTBOARD				
First Wall				
Be	2.27×10^{2}	2.23×10^{2}	2.35×10^{2}	4.58×10^{2}
Cu	2.99×10^{3}	3.00×10^{3}	2.88×10^{3}	9.12×10^{2}
SS	2.82×10^{3}	2.79×10^{3}	2.47×10^{3}	1.76×10^{3}
Vacuum Vessel	3.15	3.15	3.77	2.45

Table 8. Peak End-of-Life Tritium Production in FW and VV (appm @ 3 FPY)

	UW	UW	UW	TSI
Code	ONEDANT	ONEDANT	ONEDANT	ANISN
Evaluation	FENDL/E-1.0	FENDL/E-1.0	ENDF/B-V	FENDL/E-1.0
Processing Code	NJOY TRANSX	NJOY TRANSX	MINX AMPX,KAOS	NJOY TRANSX
Energy Groups	175n-42g	46n-21g	46n-21g	175n-42g
INBOARD				
First Wall				
Be	1.73×10^{2}	1.69×10^{2}	1.78×10^{2}	3.86×10^{2}
Cu	4.57	4.51	4.64	8.60
SS	0.92	0.92	1.57	1.15
Vacuum Vessel	1.74×10^{-5}	1.78×10^{-5}	4.69×10^{-4}	1.18×10^{-4}
OUTBOARD				
First Wall				
Be	2.27×10^{2}	2.23×10^{2}	2.35×10^{2}	4.51×10^{2}
Cu	6.37	6.29	6.46	9.84
SS	1.30	1.30	2.24	1.46
Vacuum Vessel	2.36×10^{-5}	2.41×10^{-5}	6.35×10^{-4}	1.42×10^{-4}

Table 9. Peak End-of-Life (@ 3 FPY) Magnet Radiation Effects

	UW	UW	UW	UW	TSI
Code	ONEDANT	ONEDANT	ONEDANT	ONEDANT	ANISN
Evaluation	FENDL/E-1.0	FENDL/E-1.0	ENDF/B-V	ENDF/B-V	FENDL/E-1.0
Processing Code	NJOY TRANSX	NJOY TRANSX	NJOY TRANSX	MINX AMPX,KAOS	NJOY TRANSX
Energy Groups	175n-42g	46n-21g	30n-12g	46n-21g	175n-42g
INBOARD					
Fast n fluence (E>0.1 MeV) (n/cm^2)	1.50×10^{17}	1.49×10^{17}	1.56×10^{17}	2.04×10^{17}	1.63×10^{17}
Insulator dose (eV/cm^3)	1.51×10^{22}	1.51×10^{22}	1.60×10^{22}	2.14×10^{22}	1.65×10^{22}
Cu dpa	9.65×10^{-5}	9.64×10^{-5}	1.03×10^{-4}	1.33×10^{-4}	1.06×10^{-4}
OUTBOARD					
Fast n fluence (E>0.1 MeV) (n/cm^2)	2.21×10^{16}	2.21×10^{16}	2.36×10^{16}	3.22×10^{16}	2.31×10^{16}
Insulator dose (eV/cm^3)	2.23×10^{21}	2.25×10^{21}	2.43×10^{21}	3.37×10^{21}	2.47×10^{21}
Cu dpa	1.42×10^{-5}	1.44×10^{-5}	1.56×10^{-5}	2.09×10^{-5}	1.59×10^{-5}

MAGNET RADIATION EFFECTS

Table 9 gives the peak end-of-life magnet radiation effects. This includes the fast neutron fluence (E>0.1 MeV), the absorbed dose in the organic insulator, and the displacement damage in the Cu stabilizer. The peak magnet radiation effects based on FENDL and ENDF/B-V using the same processing codes (NJOY/TRANSX) differ by less than ~8%. The peak magnet radiation effects based on FENDL with 175n-42g and 46n-21g group structures are almost identical (<1% difference). Using the same multigroup FENDL data, ANISN gives peak magnet radiation effects different from ONEDANT by less than ~12%. Comparing the results based on FENDL to those based on ENDF/B-V with the same group structure using different processing codes (MINX/AMPX), the peak end-of-life magnet radiation effects differ by as much as 50%.

SUMMARY AND CONCLUSIONS

The differences in nuclear responses calculated with FENDL and ENDF/B-V using the same processing codes (NJOY/TRANSX) are in general smaller than the differences between results

obtained using different processing codes. Comparing the results based on FENDL to those based on ENDF/B-V using the same processing codes (NJOY/TRANSX), the flux and design relevant nuclear parameters differ by <8%. The only exceptions are a 20% difference in gamma flux at the VV and a 30% difference in nuclear heating in the B_4C/Pb back layer.

The effect on nuclear heating of neglecting the decay energy associated with the short lived ($T_{1/2}$ < 1 day) radionuclides in the kerma factor is <10%. ENDF/B-V processed with MINX/AMPX/KAOS gives larger heating than FENDL processed by NJOY/TRANSX using the same group structure. The differences are large even when the effect of inclusion of decay energy is factored out. The differences can be as high as 25% in Cu, 40% in Inconel, and 60% in the magnet. Comparing the results based on FENDL to those based on ENDF/B-V with the same group structure using different processing codes (MINX/AMPX/KAOS), large differences are obtained in fluxes and design relevant nuclear parameters. In addition to large differences in nuclear heating, the most serious discrepancies are 45% in neutron flux at magnet, 17% and 60% in gamma fluxes at the FW and magnet, respectively, 22% in dpa in Inconel VV, 52% in He production in Inconel VV, 72% in T production in SS, a factor of 26 in T production in Inconel VV, and up to 50% in peak magnet radiation effects.

The difference between flux and design relevant nuclear parameters based on FENDL with the original 175n-42g group structure and a 46n-21g collapsed group structure is very small (<3%). Using the same multigroup FENDL data, ANISN gives flux, nuclear heating, and dpa results different from ONEDANT by <12%. Some of these differences could be related to the slightly different source representations used. For gas production larger differences are obtained. The most serious discrepancies include 40% and 20% in He production in the FW and Inconel VV, respectively, a factor of 3 in H production in Be and Cu of the FW, 30% in H production for Inconel VV, a factor of 2 in T production in Be and Cu of the FW and a factor of 6 in the Inconel VV. The differences are attributed to differences in gas production cross sections used. While the ANISN calculation uses REAC*3 data, the ONEDANT calculations use the partial cross section data in FENDL/MG.

Due to the observed large differences in nuclear heating and other nuclear responses calculated using data processed by NJOY and KAOS, the processing methods used need to be investigated and evaluated. Integral experiments for nuclear responses of interest to the designers will be useful to validate the processed nuclear response data. The total gas production cross sections in the FENDL library to eliminate errors that can result from leaving them to be calculated by the user by adding all possible partial cross sections provided in the library.

REFERENCES

[1] IAEA Advisory Group Meeting on "Improved Evaluations and Integral Data Testing for FENDL", Garching, Germany, September 1994; Summary Report Prepared by S. Ganesan and Published as IAEA Nuclear Data Section Report INDC(NDS)-312 (December 1994).

[2] M. Sawan, "FENDL Neutronics Benchmark: Specifications for the Calculational Neutronics and Shielding Benchmark," IAEA Nuclear Data Section Report INDC(NDS)-316 (December 1994).

[3] IAEA Specialists Meeting on the Fusion Evaluated Nuclear Data Library (FENDL), Vienna, Austria, May 1989; Summary Report Edited by V. Goulo and Published as IAEA Nuclear Data Section Report INDC(NDS)-223/GF (1989).

[4] R. MacFarlane et al., "NJOY 91.38, A Code System for Producing Pointwise and Multigroup Neutron and Photon Cross Sections from ENDF/B Evaluated Nuclear Data," PSR-171, Radiation Shielding Information Center, Oak Ridge National Laboratory (July 1992).

[5] R. MacFarlane, "TRANSX 2: A Code for Interfacing MATX Cross Section Libraries to Nuclear Transport Codes," Los Alamos National Laboratory Report, LA-12312-MS (July 1992).

[6] F. Mann and D. Lessor, "REAC*3 Nuclear Data Libraries," Nuclear Data for Science and Technology, Proc. International Conf. held at Julich, Germany, 13-17 May 1991, pp 936

[7] R. Kinsey, comp., "ENDF/B Summary Documentation," National Nuclear Data Center, Brookhaven National Laboratory Report BNL-NCS-17541 (ENDF-201), 3rd Ed., ENDF/B-V (1979).

[8] C. Weisbin et al., "MINX, A Multigroup Interpretation of Nuclear Cross Sections, Los Alamos National Laboratory Report, LA-6486-MS (1976).

[9] N. Greene et al., "AMPX: A Modular Code System for Generating Coupled Multigroup Neutron-Gamma Libraries from ENDF/B," Oak Ridge National Laboratory Report, ORNL/TM-3706 (1976).

[10] Y. Farawila, Y. Gohar and C. Maynard, "KAOS/LIB-V: A Library of Nuclear Response Functions Generated by KAOS-V Code from ENDF/B-V," Argonne National Laboratory Report ANL/FPP/TM-241 (April 1989).